Tetrahedron 67 (2011) 8740–8746

Contents lists available at SciVerse ScienceDirect

Tetrahedron

journal homepage: www.elsevier.com/locate/tet

meso-Dithiole and tetrathiafulvalene dipyrromethanes a route to metal dithiole–dipyrrin complexes and to fluorescent tetrathiafulvalene–BODIPY

Kai-Ling Huang, Nathalie Bellec, Michel Guerro, Franck Camerel, Thierry Roisnel, Dominique Lorcy *

Sciences Chimiques de Rennes, UMR 6226 CNRS, Université de Rennes 1, Campus de Beaulieu, Bât 10A, 35042 Rennes Cedex, France

ARTICLE INFO

Article history:
Received 13 July 2011
Received in revised form 29 August 2011
Accepted 8 September 2011
Available online 12 September 2011

Keywords:
Tetrathiafulvalene
Electroactive ligands
Dipyrromethanes
Dipyrrins
BODIPY

ABSTRACT

A series of *meso*-dithiole and tetrathiafulvalene (TTF) dipyrromethanes have been prepared via the reaction of the appropriate aldehyde with either pyrrole or 3-ethyl-2,4-dimethyl-pyrrole under acid catalysis. Oxidation to the corresponding *meso*-dithiole dipyrrins is reported together with the formation of the metal chelate complexes (M=Zn, Cu, Ni) as well as the *meso*-dithiole boron-dipyrromethene (BODIPY). The molecular structures of these metal (Cu, Ni) and boron complexes are presented and discussed. According to a similar strategy the *meso*-TTF BODIPY is prepared and its photophysical properties are presented and compared with those of the *meso*-dithiole BODIPY.

1. Introduction

The electroactivity of the tetrathiafulvalene (TTF) has focused a lot of attention as the leading constituent of various molecular materials, displaying a wide range of attractive applications, such as sensors, receptors, switches, and conductors.[1–4] To reach such high versatility, numerous chemical modifications have been realized on the TTF skeleton.[1–4] For example, various coordination functions have been grafted on the TTF core in order to convert the TTF into an electroactive ligand[5] for the elaboration of hybrid multifunctional materials.[6] Our ongoing interest in the synthesis and the chelating ability studies of acetylacetonate TTF derivatives (Chart 1)[7] or aza analogues prompted us to investigate dipyrrin substituted TTF. Indeed, dipyrrin derivatives are known to form, after deprotonation, stable complexes with large variety of metal ions.[8] Moreover, dipyrrin can also form after complexation in basic medium highly fluorescent boron difluoride complexes, well-known as BODIPY. Therefore the grafting of a dipyrrin functional group on the TTF core could open various perspectives for the elaboration of novel electroactive organic functional fluorophores.[8–10] A well developed route to access 5-substituted dipyrrin (Chart 1) lies on the condensation of two pyrrole on an aldehyde in the presence of an acid catalyst,[11,12] followed by an oxidation of the corresponding dipyrromethane using an oxidizing agent, such as DDQ or *p*-chloranil.[8]

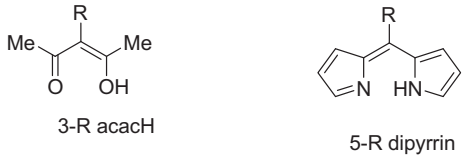

Chart 1.

Such a synthetic strategy appears compatible with the TTF chemistry and in order to graft a dipyrrin fragment on a TTF core, we have explored two different approaches: (i) functionalization of a dithiole core with a dipyrromethane group, followed by its heterocoupling with another dithiole core to form an unsymmetrically substituted TTFs, (ii) functionalization of a preformed TTF core with a carboxaldehyde group, which serves as an anchoring function to introduce the dipyrromethane fragment on the TTF cores. Oxidation of these dithiole and TTF dipyrromethane derivatives was performed and the abilities of the dipyrrin fragments to form stable metal and difluoroboron complexes were evaluated.

2. Results and discussion

2.1. Synthesis of the *meso*-substituted dipyrromethanes and associated metal and difluoroboron dipyrrin complexes

The first approach was devoted to the synthesis of two *meso*-dithiole-2-thionedipyrromethane derivatives, one where the two

* Corresponding author. Fax: +33 2 23 23 67 38; e-mail address: dominique.lorcy@univ-rennes1.fr (D. Lorcy).

0040-4020/$ – see front matter © 2011 Elsevier Ltd. All rights reserved.
doi:10.1016/j.tet.2011.09.019

pyrroles are unsubstituted **2** and a second one where the pyrroles bear three alkyl substituents **3**. For that purpose, the starting carboxaldehyde-dithiole **1** was synthesized according to literature procedure.[13] The targeted dipyrromethane-dithioles **2** and **3** were synthesized by the acid-catalyzed condensation of the carboxaldehyde-dithiole **1** with an excess of pyrrole for **2** or 3-ethyl-2,4-dimethyl-pyrrole for **3** (Scheme 1).[11] Work up of the reaction and purification by column chromatography lead to the *meso*-dithiole-2-thionedipyrromethane derivatives **2** and **3** in fair yields (53% for **2** and 36% for **3**).

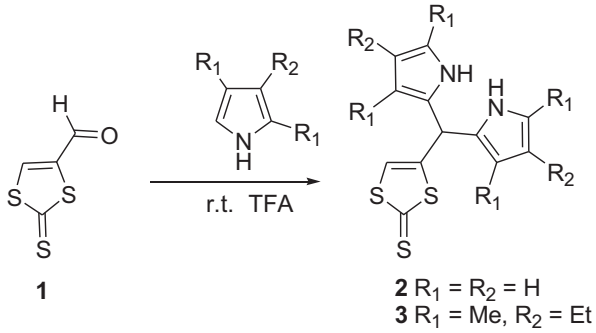

Scheme 1.

Single crystals suitable for X-ray structure analysis were obtained for dithioles **2** and **3** by slow evaporation of a concentrated dichloromethane solution. Dithioles **2** and **3** crystallize in the monoclinic system, space group $P2_1/c$ for **2** and $P2_1/a$ for **3**, with two crystallographically independent molecules in general position in each case. No significant differences have been observed between the two crystallographically independent molecules, therefore only one molecular structure of dithiole **2** and **3** are presented in Fig. 1.

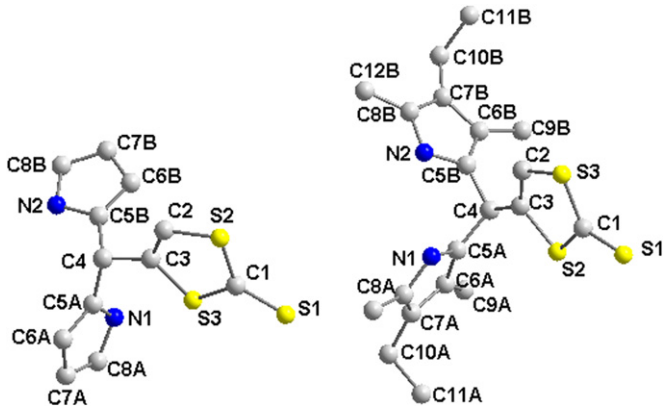

Fig. 1. Molecular structure of dipyrromethane-dithioles **2** (left) and **3** (right). (Hydrogen atoms have been removed for clarity).

On both derivatives, dithiole core and pyrrole moieties appear to be fully planar. However, the orientation of the nitrogen atoms of the pyrrole fragments is different on the two molecules. Indeed, for compound **2**, the NH point in opposite directions while for compound **3** the NH point to the same side.[14] Analysis of the bond lengths and bond angles in both derivatives **2** and **3** shows that there is no significant difference between these two types of conformers.

Dipyrromethane derivatives are well-known precursors to form dipyrrin–transition metal complexes.[8] To form metal complexes, dipyrromethane is first oxidized into a dipyrrin with an oxidizing agent, such as DDQ or *p*-Chloranil, which then reacts with divalent or trivalent salts in the presence of base. In our case, DDQ was used as oxidizing agent to generate in situ the dipyrrin.[8] Several attempts have been performed to try to isolate the dipyrrin but the compound was found to be unstable during the purification processes. Thus, directly after the oxidation of the dipyrromethane **2**, metal salt such as Ni^{2+}, Cu^{2+}, and Zn^{2+} with acetate as counter-ion were directly added into the medium. In all the cases, the bis[5-(dithiole-2-thione)-4,6-pyrrinato]M(II) complexes **4**–**6** were obtained as dark-red or dark-green precipitates (Scheme 2). It is worth mentioning that only the Zinc(II) complex **6** could be analyzed by ^{1}H NMR spectroscopy, due to the presence of a paramagnetic Ni and Cu centers.

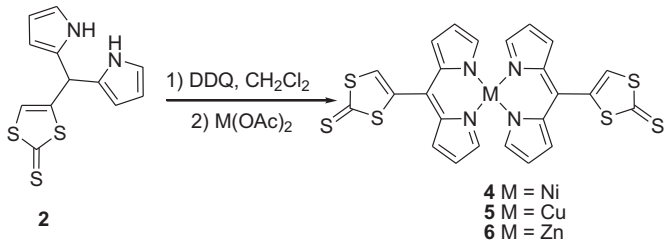

Scheme 2. Synthetic route for the preparation of the metal complexes with nickel, copper and zinc from the dipyrromethane **2**.

Single crystals suitable for X-ray structure investigations were obtained with the Ni(II) complex **4** and the Cu(II) complex **5** by slow evaporation of CH_2Cl_2 solutions. Crystal structure analyses reveal that both complexes are isostructural and crystallize in the orthorhombic system, Pnaa space group. They are mononuclear with the metal atom coordinated in a distorted tetrahedral arrangement by two dipyrrin ligands. The geometry around the metal center is not square planar, in contrary to that have been already observed in the case of acetylacetonate (acac) ligands and can be explained by steric constrains between the pyrrole fragments around the metallic center. As shown in Fig. 2, the nickel atom is coordinated by two quasi-planar dipyrrin moieties with an angle of 46.1(2)° between the two planes. The ligand bite angles, N–Cu–N 91.16(10)° and N–Ni–N 91.17(12)° are smaller than the remaining N–M–N angles (in the range 97.44(10)° for Cu complex and 97.59 (12)° for Ni complex). The Cu-N and Ni–N distances are in the same range 1.951(2)–1.957(3) Å. These distances are longer than the one observed in the related bis(*meso*-phenyl-4,6-dipyrronato)Ni complex (1.879(2) Å).[12] The Ni–N bond length appears to be closer to the one usually observed in Nickel porphyrins (1.95 Å).[15]

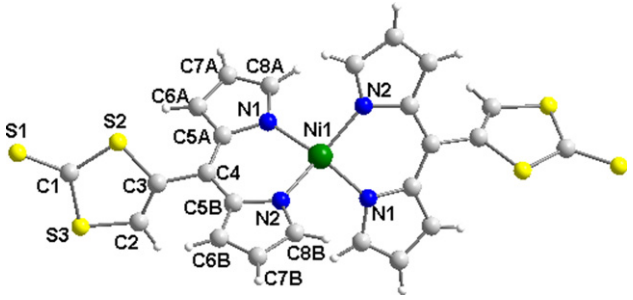

Fig. 2. Molecular structure of the Ni complex **4** with the atomic numbering.

It is also interesting to compare the evolution of the bond lengths between the dipyrromethanes **2** and **3**, and the dipyrrin within complexes **4** and **5**. In molecules **2** and **3**, the distance on the methane bridge between the two pyrrole cores are characteristic of single bonds (C–C=1.34 Å; C=C=1.51 Å) (Table 1). After oxidation and metal complexation, the distance between the carbon atoms on the methene bridge decrease and are in between the lengths of

Table 1
Selected bond lengths (Å) for **2**, **3**, **4**, **5**, and **7**

	2	**3**	**4** (M=Ni)	**5** (M=Cu)	BODIPY **7**	
M–N1			1.951 (3)	1.951 (2)	B–N1	1.556 (4)
M–N2			1.957 (3)	1.951 (3)	B–N2	1.551 (3)
C2–C3	1.336 (3)	1.347 (4)	1.331 (6)	1.330 (4)		1.338 (2)
C3–C4	1.525 (3)	1.523 (4)	1.501 (5)	1.494 (4)		1.485 (3)
C4–C5A	1.510 (2)	1.501 (4)	1.391 (6)	1.389 (4)		1.392 (3)
C4–C5B	1.511 (2)	1.506 (4)	1.393 (5)	1.405 (2)		1.408 (4)
C5A–N1	1.375 (2)	1.378 (4)	1.399 (5)	1.403 (4)		1.406 (3)
C5A–C6A	1.372 (2)	1.369 (4)	1.416 (6)	1.425 (5)		1.441 (5)
C6A–C7A	1.434 (3)	1.430 (4)	1.380 (6)	1.361 (5)		1.385 (2)
C7A–C8A	1.369 (3)	1.378 (4)	1.395 (5)	1.410 (4)		1.422 (3)
C8A–N1	1.370 (2)	1.373 (4)	1.336 (5)	1.332 (4)		1.349 (4)
C5B–N2	1.374 (2)	1.384 (3)	1.402 (4)	1.396 (4)		1.399 (2)
C5B–C6B	1.373 (2)	1.368 (4)	1.419 (6)	1.414 (4)		1.428 (4)
C6B–C7B	1.416 (3)	1.436 (4)	1.372 (6)	1.376 (5)		1.395 (3)
C7B–C8B	1.363	1.370 (4)	1.424 (6)	1.403 (5)		1.411 (3)
C8B–N2	1.387 (2)	1.373 (4)	1.340 (5)	1.340 (4)		1.358 (4)

pure single and double carbon–carbon bonds, a good indication of a delocalization between the two pyrrole cores. The lengths within the dithiole fragment are weakly affected by the oxidation and the metal complexation but a marked decrease of the distance C3–C4 between the dithiole fragment and the dipyrrin is observed. It can also be noticed that a redistribution of the bond lengths occurs on the pyrrole cores after oxidation and metal complexation.

Different views of the crystal packing of the Ni complex **4** are presented in Fig. 3. The crystal structure can be best described as formed of stacks of complexes running along the *a* axis. The long axis of the complex is rotated by 90° between two adjacent molecules along the stacks. Ni–Ni distance along the stack is 4.403(2) Å and there is no π–π stacking between the organic fragments of two neighboring molecules.

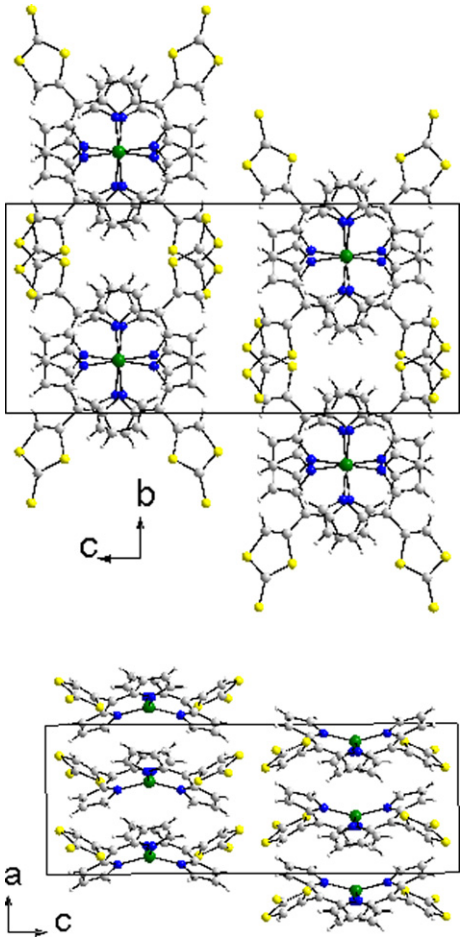

Fig. 3. Organization of bis(dipyrrinato)Ni complex **4** onto the *bc* plane (top) and onto the *ac* plane (bottom).

Being successful in the synthesis of bis(dipyrrinato) metal complexes, the synthesis of a BODIPY derivative starting from dipyrromethane dithiole **3** was investigated (Scheme 3). Indeed, *meso*-substituted BODIPY derivatives are also synthesized by oxidizing dipyrromethane skeleton with DDQ followed by the addition of $BF_3 \cdot OEt_2$ in presence of triethylamine. According to this strategy, the BODIPY **7** substituted in the *meso* position by a dithiole fragment was synthesized in 40% yield (Scheme 3).

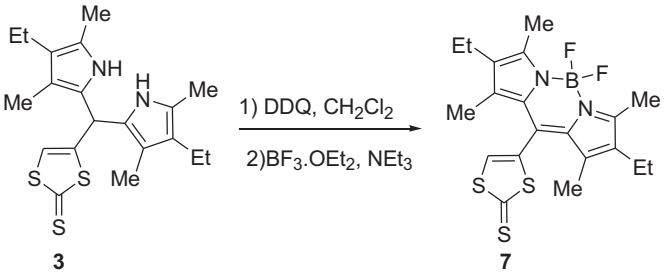

Scheme 3. Synthetic approach for the preparation of BODIPY **7** substituted in the *meso* position by a dithiole.

Single crystals of the difluoroboron complex **7**, suitable for X-ray structure analysis, were obtained by slow evaporation of a dichloromethane solution. Selected bond lengths are listed in Table 1. The molecular structure of compound **7** is presented in Fig. 4. The dithiole ring and the BODIPY core are planar and located in planes almost perpendicular to each other. Comparison of the bond lengths with those observed in the dipyrronato Ni or Cu complexes reveals that the dipyrrin moieties are weakly affected by the nature of the coordinated atom. All these structures exhibit a delocalized π-electron system on the dipyrrin fragment with a similar electron distribution.

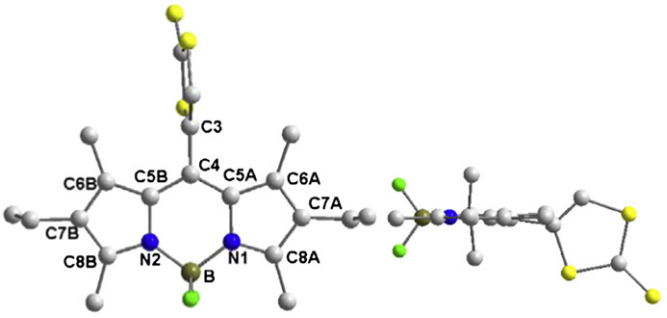

Fig. 4. Two views of the molecular structure of BODIPY **7**.

In order to form a TTF core substituted with one dipyrromethane group, the cross-coupling reaction of the dithiole **2** with 4,5-dimethylthiodithiole-2-thione in $P(OEt)_3$ at 100 °C or reflux were first investigated. However, in both cases, the formation of the targeted TTF was not observed. Cross-coupling reactions between thiones being sensitive to the nature of the exocyclic heteroatom on the dithiole rings, the 4,5-dimethylthiodithiole-2-one **8** was used as starting material (Scheme 4). Following this strategy, the unsymmetrical TTF **10** was isolated in fair yield (23%). In the same manner, by heating at 100 °C ethylene dithiodithiole-2-one **9** with dithiole **2** in distilled $P(OEt)_3$, the corresponding EDT–TTF **11** formed in 10% yield.

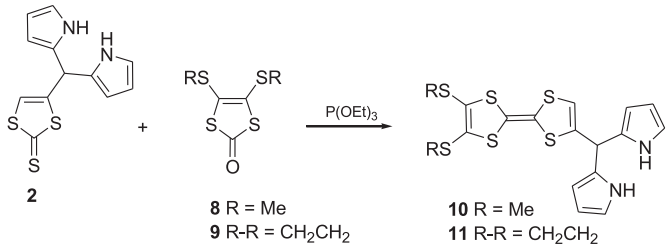

Scheme 4. Strategy used to synthesize functional TTF molecules carrying a pendent dipyrromethane fragment.

In order to improve the yields of the target molecule, the TTF derivative substituted in the *meso* position by a dipyrromethane fragment, a new synthetic way starting from the trimethylTTF–carboxaldehyde compound was investigated. This TTF derivative (Me_3TTFCHO)[16] in the presence of an excess of pyrrole and CF_3CO_2H (TFA) as catalyst leads to a mixture of two TTF isomers **12** and **13** in a very poor overall yields (Scheme 5). These isomers were identified by mass spectrometry and according to ^{1}H NMR data the desired Me_3TTF dipyrromethane **12** was the minor product.[11b] A plausible explanation for such a low yield is that TTF-aldehyde is partially decomposed in the presence of trifluoroacetic acid. Indeed, TTF are known to be sensitive to acid medium.[17] Attempts to separate these derivatives by column chromatography were unsuccessful.

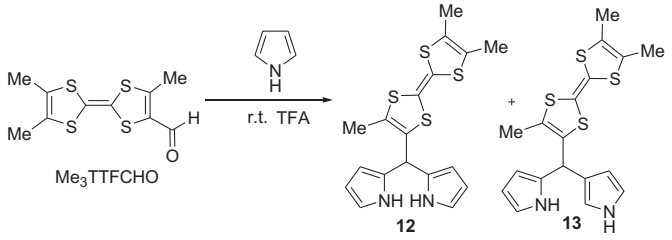

Scheme 5. Direct synthesis from trimethylTTF–carboxaldehyde compound.

Therefore, to impede the formation of the TTF β-isomer **13**, the 2,3,4-trisubstituted pyrrole was used instead of the non-substituted pyrrole. The dipyrromethane derivative **14** was synthesized by reaction of Me_3TTFCHO with an excess of 2,4-dimethyl-3-ethyl-pyrrole catalyzed by trifluoroacetic acid at room temperature. The excess of the pyrrole derivative was removed upon reduced pressure and attempt to isolate TTF **14** in pure form were unsuccessful, therefore crude TTF **14** was directly oxidized into the corresponding dipyrrin with DDQ and reacted with $BF_3{\cdot}OEt_2$ in presence of NEt_3 to form the TTF–BODIPY **15**. Using this strategy, TTF **15** was obtained as purple powder in 15% yield (Scheme 6).

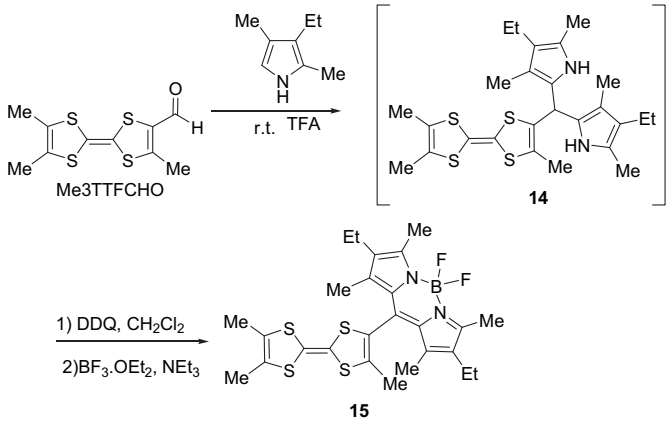

Scheme 6. Procedure for the synthesis of a BODIPY substituted in the *meso* position by a TTF fragment.

2.2. Electrochemical and optical investigations

The redox behavior of the TTF **10**, **11**, and **15** was investigated by cyclic voltammetry in dichloromethane and their oxidation potentials are listed in Table 2. Two reversible monoelectronic processes were observed as the typical signature of the electroactive TTF cores. The two successive waves correspond to the oxidation of the TTF into its radical cation and to the formation of the dication, respectively. In addition, for TTF **15**, two additional redox processes were observed on the cyclic voltammogram. Indeed, the BODIPY is an ambipolar molecule, which can be oxidized into a cation radical or reduced into a radical anion.[18] To evaluate the influence of the TTF core on the redox properties of the BODIPY fragment in molecule **15**, the electrochemical properties of BODIPY **7** were also investigated. Both derivatives exhibit an irreversible oxidation wave corresponding to the oxidation of the BODIPY into its radical cation. Investigation of these compounds in another solvent, such as acetonitrile does not modify the irreversible shape of this redox processes. This process occurs at 1.32 V versus SCE for the dithiole **7**, while it is observed at higher potential for the TTF **15**. This is assigned to the presence of the TTF dication, which acts as an electron acceptor and the oxidation of the BODIPY is anodically shifted. Similarly, a noticeable influence of the TTF core can be observed on the reduction of the BODIPY into its radical anion species. For both derivatives, an irreversible reduction wave is observed at −1.03 V for **7** and at −1.1 V for TTF **15**. This cathodic shift is due to the fact that the electron rich TTF core in **15** renders the BODIPY moiety more difficult to reduce.

Table 2
Electrochemical data

Compound	E_{red}BODIPY	$E^1_{1/2}$ TTF	$E^2_{1/2}$ TTF	E_{ox}BODIPY
TTF **10**	—	0.41	0.87	
TTF **11**	—	0.42	0.87	
BODIPY **7**	−1.03rev	—	—	1.32irr
TTF **15**	−1.1irr	0.38	0.92	1.40irr

E in V versus SCE, CH_2Cl_2 0.1 M, Pt working electrode with 0.1 M *n*-Bu_4NPF_6 scanning rate100 mV/s.

The UV–vis absorption spectra of BODIPY **7** and TTF–BODIPY **15** have been recorded in CH_2Cl_2 and spectroscopic data are gathered in Table 3. The compounds show similar absorption patterns, which are characteristic of BODIPY fluorophores and measured absorption, excitation and emission spectra are presented in Fig. 5. The absorption spectrum is composed of a strong $S_0 \rightarrow S_1$ ($\pi \rightarrow \pi^*$) transition located around 545 nm, with high molar extinction coefficients (Table 3). A second absorption band centered around 370 nm, is assigned to the $S_0 \rightarrow S_2$ transition of the BODIPY subunit.[19] The third absorption around 238 nm is likely due to $\pi-\pi^*$ transitions localized on the dipyrrin fragments. The discrepancy observed between the molar extinction coefficient of compound **7** and **15** at 545 and 380 nm is attributed to the contribution of the dithiole fragment,

Table 3
Optical data measured in dichloromethane solution at 298 K

Compound	λ_{abs} (nm)	ε (M^{-1} cm^{-1})	λ_F (nm)	Φ_F[a]
TTF	443	540	—	—
	365	2290		
	313	13,190		
BODIPY **7**	549	56,100	567	0.38
	375	16,970		
	237	22,820		
TTF **15**	545	38,960	581	0.43
	385	7075		
	329	8400		
	239	18,870		

[a] Determined in dichloromethane solution (**7**, $c=1.2\times10^{-6}$ M; **15**, $c=4.0\times10^{-6}$ M) using Rhodamine 6G as reference (Φ_F=0.78 in water, λ_{exc}=488 nm).[20]

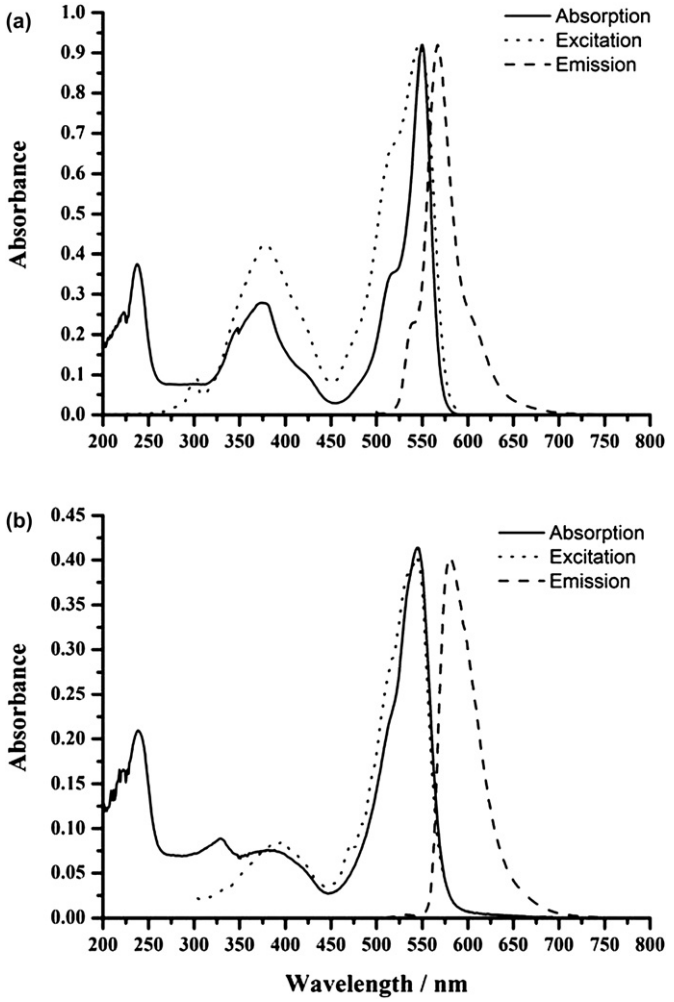

Fig. 5. Absorption, excitation and emission spectra of BODIPY **7** (C=1.64×10^{-5} M) (up) and TTF–BODIPY **15** (C=1.06×10^{-5} M) (down).

which absorb in this area (for instance for compound **3** $\lambda_{abs}(\varepsilon)$ 539 (7020) and 370 (8050)). An additional absorption band is observed with compound **15** at 329 nm and is attributed to π–π* transitions localized on the TTF core (see unsubstituted TTF Table 3).

The two BODIPY derivatives have high fluorescence quantum yields around 40%. The weak Stokes' shifts (about 500–1000 cm^{-1}) observed over the whole series of fluorophores is in good agreement with a singlet emitting state. Excitation spectra perfectly match absorption spectra, which is in keeping with a unique excited state, excluding the existence of a CT transition, despite the presence of electron-donating fragments on these fluorophores. All fluorescence spectra exhibit nice mirror symmetry with the lowest energy absorption band, meaning that the corresponding transitions involve the same excited state. For all the above spectroscopic data, no influence of the *meso*-substitution either by a dithiole or a TTF fragment can be noticed. These results confirm that the optical properties are weakly affected by the nature of the substituent in the *meso* position.

However, this result is rather surprising as in all the cases reported so far where a TTF is connected to a fluorophore, a quenching of the fluorescence is observed. Indeed, the fluorescence of various fluorophore unit, such as phthalocyanine[21] porphyrin,[22] perylene diimide,[23] anthracene,[24] pyrene[25] 5-methoxy-2-(2-pyridil)thiazole,[26] and iridium complex,[27] was either completely or partially quenched due to an electron transfer from the grafted neutral TTF moiety to the excited fluorophore unit. In these cases the fluorescence was recovered after the removal of one electron from the TTF unit leading to redox-fluorescent switches. Therefore we decided to investigate the influence of the chemical oxidation of the TTF core of the TTF–BODIPY **15** on the fluorescence intensity. This was realized by adding an increasing amount of $Fe(ClO_4)_3$ or $NOPF_6$, as oxidizing agent, to a solution of BODIPY–TTF **15**. Interestingly, in both cases no enhancement or decrease of the fluorescence intensity was observed. We also investigated the intermolecular influence of the Me_3-TTF on the fluorescence of the BODIPY **7**. This was realized by adding an increasing amount of Me_3-TTF to a solution of BODIPY **7** in CH_2Cl_2 (C=1.64×10^{-5} M). In that case, even after the addition of 100 equiv of Me_3-TTF to the BODIPY solution no quenching of the fluorescence was observed. Therefore, in our case, the redox active fluorophore conserves its fluorescent behavior independently of the redox state of the TTF. It is interesting to note that in BODIPY–TTF **15**, the TTF core lies in a plane perpendicular to the one formed by the BODIPY moiety, as for the dithiole core in BODIPY **7** (Fig. 4), and therefore held the TTF moiety in a configuration which prevents through space intermolecular interactions.

3. Conclusions

In summary, we have synthesized new dithiole and TTF derivatives bearing a dipyrromethane moiety. We have demonstrated that they can form either bis(dipyrrinato) metal complexes or boron difluoride dipyrrinato complexes. The photophysical behavior of the *meso*-dithiole–BODIPY and *meso*-TTF–BODIPY were found to be very similar and no quenching of the fluorescence was observed due to the presence of a neutral TTF. Therefore, a new redox active fluorophore based on TTF displaying a unique behavior was rationally designed. Further investigations will be devoted to the elaboration of other BODIPY–TTF in order to study their potential as precursor of conducting fluorescent materials.

4. Experimental

4.1. General

^{1}H NMR, ^{13}C NMR ^{11}B NMR, and ^{19}F NMR spectra were recorded on a Bruker Avance 300 III spectrometer with tetramethylsilane as internal reference using $CDCl_3$ as solvent unless otherwise stated. Chemical shifts are reported in parts per million. Mass spectra and elemental analysis results were performed by the Centre Régional de Mesures Physiques de l'Ouest (CRMPO) in Rennes. Melting points were measured using a Kofler hot stage apparatus and are uncorrected. Cyclic voltammetry were carried out on a 10^{-3} M solution of the compounds in dichloromethane, containing 0.1 M n-Bu_4NPF_6 as supporting electrolyte. Voltammograms were recorded at 0.1 Vs^{-1} on a platinum disk electrode (A=1 mm^2). The potentials were measured versus Saturated Calomel Electrode. FT-IR spectra were recorded using a VARIAN 640-IR using a PIKE Technologies MIRacle(TM) ATR (single Attenuated Total Reflectance) with a diamond crystal. UV–vis spectra were recorded using a Cary 100 UV–vis spectrophotometer (Varian). Me_3TTFCHO was prepared according to published procedure.[16] Photoluminescence spectra were recorded with a PTI spectrofluorimeter (PTI-814 PDS, MD 5020, LPS 220B) using a Xenon lamp. All the reagents were purchased and used without additional purification.

4.2. Synthesis and characterization

4.2.1. Synthesis of TTF of 5-(dithiole-2-thione)dipyrromethane ***2***. Freshly distilled pyrrole (8.9 mL, 0.128 mol) and dithiole **1** (700 mg, 4.3 mmol) were mixed into a 25 mL flask, and the reaction mixture was degassed for 10 min by bubbling Ar. TFA (32 μL, 0.43 mmol) was added and the medium was stirred for 10 min

under a current of Ar. A solution of NaOH (4.9 mL of 0.1 M) was added. The solution was afterward extracted with ethyl acetate, washed with water, dried over $MgSO_4$, and then ethyl acetate and pyrrole were evaporated under vacuum. Addition of MeOH to the residue allowed the formation of a yellow-green precipitate, which is recrystallized in CH_2Cl_2 to afford dithiole **2** in 53% yield; Mp=143 °C; ^{1}H NMR ($CDCl_3$, 300 MHz) δ 5.48 (s, 1H, CH), 6.14 (m, 2H, CH), 6.23 (m, 2H, CH), 6.66 (s, 1H, CH), 6.77 (m, 2H, CH), 8.07 (br, 2H, NH); ^{13}C NMR ($CDCl_3$, 75 MHz) δ 40.4, 108.1, 109.0, 118.5, 124.6, 128.3, 148.4, 213.2; HRMS calcd for [2M+Na] $C_{24}H_{20}N_4NaS_6$ 578.9910. Found 578.9917. Anal. calcd for $C_{12}H_{10}N_2S_3$: C, 51.77; H, 3.62; N, 10.06; S, 34.55. Found: C, 51.64; H, 3.67; N, 10.16; S, 34.68.

*4.2.2. Synthesis of 3-ethyl-5-(dithiole-2-thione)-2,4-dimethyldipyrromethane **3**.* Dithiole **1** (160 mg, 1 mmol) and 3-ethyl-2, 4-dimethyl-pyrrole (1.35 mL, 10 mmol) were mixed in a 10 mL flask and degassed for 10 min by bubbling Ar. After the addition of TFA (10 μL, 0.14 mmol), the reaction mixture was stirred for 20 min under Ar. A solution of NaOH (1 mL of 0.1 M) and ethyl acetate was added to the reaction mixture. The organic phase was washed with water (3×10 mL), dried over $MgSO_4$, and concentrated under reduced pressure. The residue was chromatographied over silica gel column using CH_2Cl_2/pentane (25/75). The dipyromethane **3** was obtained as yellow crystals in 36% yield; Mp=50 °C (dec); ^{1}H NMR ($CDCl_3$, 300 MHz) δ 1.08 (t, 6H, CH_3), 1.96 (s, 6H, CH_3), 2.17 (m, 6H, CH_3), 2.39 (q, 4H, CH_2), 5.34 (s, 1H, CH), 6.54 (s, 1H, CH), 7.54 (br, 2H, NH); ^{13}C NMR ($CDCl_3$, 75 MHz) δ 9.3, 11.2, 15.6, 17.6, 37.3, 114.9, 121.4, 121.5, 122.7, 123.9, 150.8, 214.6; HRMS calcd for $C_{20}H_{25}N_2S_3$ 389.1179. Found 389.1183.

*4.2.3. General procedure for the synthesis of bis[5-(dithiole-2-thione)-4,6-pyrrinato]M(II) complexes **4**–**6**.* To a solution of dipyrromethane **2** (140 mg, 0.5 mmol) in 20 mL CH_2Cl_2 was added DDQ (114 mg, 0.5 mmol) and the solution was stirred for 10 min at room temperature. $M(OAc)_2$, xH_2O (0.75 mmol) (M=Ni, Cu, Zn) was added to the reaction mixture as a solid and the mixture was stirred for 12 h. The precipitate was filtrated and dried under vacuum to give complexes **4**, **5**, and **6** in 30%, 25% and 20% yield, respectively. Crystals were grown by slow evaporation of a dichloromethane solution of **4** (mp >260 °C) and **5** (mp >260 °C). Bis [5-(dithiole-2-thione)-4,6-pyrrinato]Zn **6** mp >260 °C; ^{1}H NMR ($CDCl_3$, 300 MHz) δ 6.53 (dd, J=1.2 and 4.2 Hz, 4H), 7.33 (d, J=4.2 Hz, 4H), 7.59 (m, 4H), 7.71 (s, 2H); HRMS calcd for $C_{24}H_{14}N_4S_6Zn$ 613.8834. Found 613.8846.

*4.2.4. Synthesis 8-[5-(dithiole-2-thione)-4,6-pyrrinato] BODIPY **7**.* To a solution of dithiole-2-thione (310 mg, 0.8 mmol) in 15 mL of toluene DDQ (180 mg, 0.8 mmol) was added. The reaction mixture was stirred for 15 min and NEt_3 (0.4 g, 4.0 mmol) and $BF_3{\cdot}OEt_2$ (1.14 g, 8.0 mmol) were added. The solution was stirred for 30 min at room temperature and $Na_2S_2O_4$ was added. The solution was washed with water and dried over $MgSO_4$. The organic solvent was evaporated under reduced pressure and the residue was purified by column chromatography on silica gel using CH_2Cl_2 as eluent to afford **7** as a pink powder in 40% yield. Mp=90 °C; ^{1}H NMR ($CDCl_3$, 300 MHz): δ 0.96 (t, 6H, CH_3), 1.98 (s, 6H, CH_3), 2.30 (q, 4H, CH_2), 2.45 (s, 6H, CH_3), 6.88 (s, 1H, CH); ^{13}C NMR ($CDCl_3$, 75 MHz) δ 11.8, 12.7, 14.5, 17.0, 125.4, 127.9, 130.6, 134.1, 137.6, 138.4, 156.3, 212.1; ^{11}B NMR ($CDCl_3$, 96 MHz) δ 0.56 (t, J_{B-F}=33 Hz); ^{19}F($CDCl_3$, 282 MHz) δ −145.6 (q, J_{B-F}=33 Hz); HRMS calcd for $[M+Na]^+$ $C_{20}H_{23}N_2F_2BNaS_3$ 459.0976. Found 459.0978.

*4.2.5. General procedure for the synthesis of TTF **10** and **11**.* Synthesis of TTF **10** and **11**: To a stirred solution of **2** (140 mg, 0.5 mmol) in 8 mL of distilled triethylphosphite was added 1 mmol of the corresponding dithiole-2-one. The reaction mixture was heated to 100 °C for 3h and the solvent was removed under vacuum. The TTFs were purified by column chromatography on silica gel using CH_2Cl_2/pentane (5:1) as eluent. TTF **10** was obtained as a light brown powder in 23% yield. Mp=60 °C; ^{1}H NMR (300 MHz, $CDCl_3$): δ 2.42 (s, 3H, CH_3), 2.44 (s, 3H, CH_3), 5.23 (s, 1H, CH), 6.03 (s, 1H, CH), 6.12 (m, 2H, CH), 6.20 (m, 2H, CH), 6.74 (m, 2H, CH), 8.04 (br s, 2H, NH); ^{13}C NMR ($CDCl_3$, 75 MHz) δ 19.2, 19.3, 40.3, 106.6, 107.7, 108.7, 115.4, 115.5, 117.9, 127.2, 127.7, 129.0, 137.8; HRMS calcd for $C_{17}H_{16}N_2S_6$ 439.9637. Found 439.9634. TTF **11** was obtained as a light brown powder in 10% yield. Mp=86 °C; ^{1}H NMR (300 MHz, DMSO): δ 3.36 (s, 4H, CH_2), 5.20 (s, 1H, CH), 5.86 (m, 2H, CH), 5.94 (m, 2H, CH), 6.19 (s, 1H, CH), 6.66 (m, 2H, CH), 10.73 (br s, 2H, NH); ^{13}C NMR (DMSO, 75 MHz) δ 30.0, 40.1, 101.4, 106.7, 107.6, 113.2, 113.3, 115.2, 117.9, 120.0, 130.3, 139.8; HRMS calcd for $C_{17}H_{14}N_2S_6$ 437.9481. Found 437.9485.

*4.2.6. General procedure for the synthesis of TTF **12** and **13**.* Pyrrole (1.5 mL, 20 mmol) and Me_3TTFCHO (200 mg, 0.72 mmol) were placed in a 10 mL flask, and degassed for 5 min by bubbling N_2. TFA (5,4 μL, 0.072 mmol) was added and the reaction mixture was stirred for 10 min under inert atmosphere. A solution of NaOH (0.7 mL 0.1 M) was added and the reaction mixture was extracted with ethyl acetate. The organic phase was washed with water, dried over $MgSO_4$, and the solvent and pyrrole were evaporated under reduced pressure. Purification by column chromatography (CH_2Cl_2) of the reaction mixture leads to an inseparable mixture of the two isomers. ^{1}H NMR of the desired TTF **12** (200 MHz, acetone-d_6): δ=1.91 (s, 3H, CH_3), 1.97 (s, 3H, CH_3), 2.07 (s, 3H, CH_3), 5.66 (s, 1H, CH), 6.16 (m, 2H, CH), 6.59 (m, 2H, CH), 6.83 (m, 2H, CH), 10.05 (br s, 2H, NH). ^{1}H NMR of the isomer TTF **13** (200 MHz, acetone-d_6): δ=1.90 (s, 3H, CH_3), 1.96 (s, 3H, CH_3), 2.07 (s, 3H, CH_3), 5.30 (m, 1H, CH), 5.98 (t, 1H, CH), 6.12 (m, 1H, CH), 6.30 (m, 1H, CH), 6.45 (s, 1H, CH), 6.76 (t, 1H, CH), 6.82 (m, 1H, CH), 10.01 (br s, 1H, NH), 10.30 (br s, 1H, NH); HRMS calcd for $C_{18}H_{18}N_2S_4$ 390.0353. Found 390.0351.

*4.2.7. Synthesis of TTF–BODIPY **15**.* Me_3TTFCHO (274 mg, 1 mmol) and 3-ethyl-2,4-dimethyl-pyrrole (1.35 mL, 10 mmol) were mixed in a 10 mL flask and degassed for 15 min by bubbling N_2. TFA (7.4 μL, 0.1 mmol) was added and the reaction mixture was stirred for 10 min under inert atmosphere after what the medium became homogeneous. The reaction mixture was stirred for an additional 20 min and NaOH (0.1 M) was added, the reaction mixture was extracted with ethyl acetate. The organic phase was washed with water, dried over $MgSO_4$, and the solvent as well as the excess pyrrole were evaporated under reduced pressure (70 °C/0.5 mbar). The residue was dissolved in 10 mL of toluene and DDQ (160 mg, 0.7 mmol) was added and the reaction mixture was stirred for 15 min. NEt_3 (0.5 g, 5 mmol) and $BF_3{\cdot}OEt_2$ (1.4 g, 10 mmol) were added and the solution was stirred for 30 min. In order to reduce the TTF core, $Na_2S_2O_4$ (1 g) was added to the medium. The organic phase was washed 2×20 mL with water, dried over $MgSO_4$, and concentrated under vacuum. The residue was chromatographied over a silica gel column using dichloromethane/pentane (1/2) as eluent. TTF **15** was obtained as purple powder 15% yield. Mp=160 °C; ^{1}H NMR (300 MHz, $CDCl_3$): δ 1.04 (t, 6H, CH_3), 1.86 (s, 3H, CH_3), 1.94 (d, 3H, CH_3), 1.96 (d, 3H, CH_3), 2.18 (s, 6H, CH_3), 2.36 (q, 4H, CH_2), 2.50 (s, 6H, CH_3); ^{13}C NMR ($CDCl_3$, 75 MHz) δ 9.3, 11.2, 12.5, 12.6, 13.7, 14.4, 14.5, 14.6, 17.1, 17.2, 110.6, 118.5, 121.0, 122.8, 123.2, 128.7, 129.6, 130.6, 131.6, 132.3, 133.1, 136.6, 137.9, 154.6, 155.1; ^{11}B NMR ($CDCl_3$, 96 MHz) δ 0.63 (t, J_{B-F}=34 Hz); ^{19}F($CDCl_3$, 282 MHz) δ −145.7 (q, J_{B-F}=34 Hz); HRMS calcd for $C_{26}H_{31}BF_2N_2S_4$ 548.14257. Found 548.1429.

4.3. Crystallography

Single-crystal diffraction data were collected on APEX II Bruker AXS diffractometer, Mo Kα radiation (λ=0.71073 Å), for compounds

2, **3**, **4**, **5** and **7** (Centre de Diffractométrie X, Université de Rennes, France). The structures were solved by direct methods using the SIR97 program,[28] and then refined with full-matrix least-square methods based on F^2 (SHELX-97)[29] with the aid of the WINGX program.[30] All non-hydrogen atoms were refined with anisotropic atomic displacement parameters. H atoms were finally included in their calculated positions.

Crystal data for **2**: ($2(C_{12}H_{10}N_2S_3)$); M=556.8, T=100(2) K; monoclinic $P2_1/c$, a=12.2422(6), b=10.6100(5), c=18.5940(8) Å, β=98.613(2)°, V=2387.93(19) Å^3, Z=4, d=1.549 g cm^{-3}, μ=0.596 mm^{-1}. A final refinement on F^2 with 5454 unique intensities and 283 parameters converged at $wR(F^2)$=0.0822 ($R(F)$=0.0343) for 5063 observed reflections with $I>2\sigma(I)$.

Crystal data for **3**: ($2(C_{20}H_{26}N_2S_3)$); M=781.22, T=100(2) K; monoclinic $P2_1/a$, a=15.0830(19), b=14.882(2), c=19.198(2) Å, β=106.965(5)°, V=4121.8(9) Å^3, Z=4, d=1.259 g cm^{-3}, μ=0.365 mm^{-1}. A final refinement on F^2 with 9420 unique intensities and 463 parameters converged at $wR(F^2)$=0.1147 ($R(F)$=0.0642) for 6639 observed reflections with $I>2\sigma(I)$.

Crystal data for **4**: ($C_{24}H_{14}N_4Ni_1S_6$); M=609.46, T=100(2) K; orthorhombic Pnaa, a=8.806(2), b=11.169(2), c=24.303(5) Å, V=2390.3(8) Å^3, Z=4, d=1.694 g cm^{-3}, μ=1.360 mm^{-1}. A final refinement on F^2 with 2741 unique intensities and 159 parameters converged at $wR(F^2)$=0.0948 ($R(F)$=0.0499) for 1495 observed reflections with $I>2s(I)$.

Crystal data for **5**: ($C_{24}H_{14}CuN_4S_6$); M=614.29, T=100(2) K; orthorhombic Pnaa, a=8.7778(12), b=11.2373(13), c=24.155(4) Å, V=2382.6(6) Å^3, Z=4, d=1.712 g cm^{-3}, μ=1.466 mm^{-1}. A final refinement on F^2 with 2739 unique intensities and 159 parameters converged at $wR(F^2)$=0.1065 ($R(F)$=0.0461) for 2446 observed reflections with $I>2\sigma(I)$.

Crystal data for **7**: ($C_{20}H_{23}BF_2N_2S_3$); M=436.39, T=150(2) K; monoclinic $P2_1/c$, a=10.114(2), b=17.514(3), c=12.206(3) Å, β=104.762(8)°, V=2090.8(8) Å^3, Z=4, d=1.386 g cm^{-3}, μ=0.381 mm^{-1}. A final refinement on F^2 with 4725 unique intensities and 259 parameters converged at $wR(F^2)$=0.0942 ($R(F)$=0.0372) for 3984 observed reflections with $I>2\sigma(I)$.

5. Supplementary data

Crystallographic data for structural analysis have been deposited with the Cambridge Crystallographic Data Centre, CCDC no 832433–832437 for compounds **2**, **3**, **4**, **5**, and **7**. Copies of this information may be obtained free of charge from The CCDC, 12 Union road, Cambridge CB2 1EZ, UK (fax: +44 1223 336033; e-mail: deposit@ccdc.cam.ac.uk or www: http://www.ccdc.cam.ac.uk).

References and notes

1. Canevet, D.; Sallé, M.; Zhang, G.; Zhang, D.; Zhu, D. *Chem. Commun.* **2009**, 2245–2269.
2. Special issue on "Molecular conductors" Batail, P. *Chem. Rev.* **2004**, *104*, 4887–5781.
3. (a) Coskun, A.; Spruell, J. M.; Barin, G.; Fahrenbach, A. C.; Forgan, R. S.; Colvin, M. T.; Carmieli, R.; Benítez, D.; Tkatchouk, E.; Friedman, D. C.; Sarjeant, A. A.; Wasielewski, M. R.; Goddard, W. A.; Stoddart, J. F. *J. Am. Chem. Soc.* **2011**, *133*, 4538–4547; (b) Klajn, R.; Stoddart, J. F.; Grzybowski, B. A. *Chem. Soc. Rev.* **2010**, *39*, 2203–2237.
4. (a) Bryce, M. R. *J. Mater. Chem.* **2000**, *10*, 589–598; (b) Nielsen, M. B.; Lomholt, C.; Becher, J. *Chem. Soc. Rev.* **2000**, *29*, 153–164; (c) Segura, J. L.; Martín, N. *Angew. Chem., Int. Ed.* **2001**, *40*, 1372–1409; (d) Martín, N.; Sanchez, L.; Herranz, M. A.; Illescas, B.; Guldi, D. M. *Acc. Chem. Res.* **2007**, *40*, 1015–1024.
5. Lorcy, D.; Bellec, N.; Fourmigué, M.; Avarvari, N. *Coord. Chem. Rev.* **2009**, *253*, 1398–1438.
6. (a) Pointillart, F.; Le Gal, Y.; Golhen, S.; Cador, O.; Ouahab, L. *Inorg. Chem.* **2009**, *48*, 4631–4633; (b) Murata, T.; Morita, Y.; Yakiyama, Y.; Fukui, K.; Yamochi, H.; Saito, G.; Nakasuji, K. *J. Am. Chem. Soc.* **2007**, *129*, 10837–10846; (c) Coronado, E.; Day, P. *Chem. Rev.* **2004**, *104*, 5419–5448.
7. (a) Bellec, N.; Lorcy, D. *Tetrahedron Lett.* **2001**, *42*, 3189–3191; (b) Massue, J.; Bellec, N.; Chopin, S.; Levillain, E.; Roisnel, T.; Clérac, R.; Lorcy, D. *Inorg. Chem.* **2005**, *44*, 8740–8748; (c) Bellec, N.; Massue, J.; Roisnel, T.; Lorcy, D. *Inorg. Chem. Commun.* **2007**, *10*, 1172–1176; (d) Fourie, F.; Swarts, J. C.; Lorcy, D.; Bellec, N. *Inorg. Chem.* **2010**, *49*, 952–959; (e) Guerro, M.; Roisnel, T.; Lorcy, D. *Tetrahedron* **2009**, *65*, 6123–6127; (f) Guerro, M.; To Uyen, D.; Bakhta, S.; Kolli, B.; Roisnel, T.; Lorcy, D. *Tetrahedron* **2011**, *67*, 3427–3433.
8. Wood, T. E.; Thompson, A. *Chem. Rev.* **2007**, *107*, 1831–1861.
9. Treibs, A.; Kreuzer, F. H. *Justus Liebigs Ann. Chem.* **1968**, *718*, 208–223.
10. (a) Ulrich, G.; Ziessel, R.; Harriman, A. *Angew. Chem., Int. Ed.* **2008**, *47*, 1184–1201; (b) Ziessel, R.; Ulrich, G.; Harriman, A. *New J. Chem.* **2007**, *31*, 496–501.
11. (a) Lee, C. H.; Lindsey, J. S. *Tetrahedron* **1994**, *50*, 11427–11440; (b) Littler, B. J.; Miller, M. A.; Hung, C. H.; Wagner, R. W.; O'Shea, D. F.; Boyle, P. D.; Lindsey, J. S. *J. Org. Chem.* **1999**, *64*, 1391–1396; (c) Gryko, D.; Lindsey, J. S. *J. Org. Chem.* **2000**, *65*, 2249–2252; (d) Rao, P. D.; Littler, B. J.; Geier, G. R., III; Lindsey, J. S. *J. Org. Chem.* **2000**, *65*, 1084–1092.
12. Brückner, C.; Karunaratne, V.; Rettig, S. J.; Dolphin, D. *Can. J. Chem.* **1996**, *74*, 2182–2193.
13. Garner, P.; Park, J. M. *J. Org. Chem.* **1987**, *52*, 2361–2364.
14. Aleśković, M.; Basarić, N.; Mlinarić-Majerski, K.; Molčanov, K.; Kojić-Prodić, B.; Kesharwani, M. K.; Ganguly, B. *Tetrahedron* **2010**, *66*, 1689–1698.
15. Jentzen, W.; Turowska-Tyrk, I.; Scheidt, W. R.; Shelnutt, J. A. *Inorg. Chem.* **1996**, *35*, 3559–3567.
16. Moore, A. J.; Bryce, M. R.; Batsanov, A. S.; Cole, J. C.; Howard, J. A. K. *Synthesis* **1995**, 675–682.
17. Giffard, M.; Alonso, P.; Garin, J.; Gorgues, A.; Nguyen, T. P.; Richomme, P.; Robert, A.; Roncali, J.; Uriel, S. *Adv. Mater.* **1994**, *6*, 298–300.
18. Bonardi, L.; Kanaan, H.; Camerel, F.; Jolinat, P.; Retailleau, P.; Ziessel, R. *Adv. Funct. Mater.* **2008**, *18*, 401–413.
19. Karolin, J.; Johansson, LB.-A.; Strandberg, L.; Ny, T. *J. Am. Chem. Soc.* **1994**, *116*, 7801–7806.
20. Olmsted, J. *J. Phys. Chem.* **1979**, *83*, 2581–2584.
21. (a) Wang, C.; Bryce, M. R.; Batsanov, A. S.; Stanley, C. F.; Beeby, A.; Howard, J. A. K. *J. Chem. Soc., Perkin Trans. 2* **1997**, 1671–1678; (b) Farren, C.; Christensen, C. A.; FitzGerald, S.; Bryce, M. R.; Beeby, A. *J. Org. Chem.* **2002**, *67*, 9130–9139.
22. (a) Li, H.; Jeppesen, J. O.; Levillain, E.; Becher, J. *Chem. Commun.* **2003**, 846–847; (b) Sadaike, S.-I.; Takimiya, K.; Aso, Y.; Otsubo, T. *Tetrahedron Lett.* **2003**, *44*, 161–165; (c) Xiao, X.; Xu, W.; Zhang, D.; Xu, H.; Lu, H.; Zhu, D. *J. Mater. Chem.* **2005**, *15*, 2557–2561; (d) Poddutoori, P. K.; Dion, A.; Yang, S.; Pilkington, M.; Wallis, J. D.; van der Est, A. *J. Porphyrins Phthalocyanines* **2010**, *14*, 178–187.
23. (a) Guo, X.; Zhang, D.; Zhang, H.; Fan, Q.; Xu, W.; Ai, X.; Fan, L.; Zhu, D. *Tetrahedron* **2003**, *59*, 4843–4850; (b) Leroy-Lhez, S.; Baffreau, J.; Perrin, L.; Levillain, E.; Allain, M.; Blesa, M.-J.; Hudhomme, P. *J. Org. Chem.* **2005**, *70*, 6313–6320; (c) Jaggi, M.; Blum, C.; Dupont, N.; Grilj, J.; Liu, S.-X.; Hauser, J.; Hauser, A.; Decurtins, S. *Org. Lett.* **2009**, *11*, 3096–3099.
24. Zhang, G.; Zhang, D.; Guo, X.; Zhu, D. *Org. Lett.* **2004**, *6*, 1209–1212.
25. Xiao, X.; Xu, W.; Zhang, D.; Xu, H.; Lu, H.; Zhu, D. *New J. Chem.* **2005**, *29*, 1291–1294.
26. (a) Fang, C.-J.; Zhu, Z.; Sun, W.; Xu, C.-H.; Yan, C.-H. *New J. Chem.* **2007**, *31*, 580–586; (b) Sun, W.; Xu, C.-H.; Fang, C.-J.; Yan, C.-H. *J. Phys. Chem. C* **2008**, *112*, 16973–16983.
27. Xu, C.-H.; Sun, W.; Zhang, C.; Zhou, C.; Fang, C.-J.; Yan, C.-H. *Chem.—Eur. J.* **2009**, *15*, 8717–8721.
28. Altomare, A.; Burla, M. C.; Camalli, M.; Cascarano, G.; Giacovazzo, C.; Guagliardi, A.; Moliterni, A. G. G.; Polidori, G.; Spagna, R. *J. Appl. Crystallogr.* **1999**, *32*, 115–119.
29. Sheldrick, G. M. *Acta Crystallogr.* **2008**, *A64*, 112–122.
30. Farrugia, L. J. *J. Appl. Crystallogr.* **1999**, *32*, 837–838.